

## 苯乙烯协助水热制备高催化活性 ZnO 管

邵 谦\* 杨梦晨 葛圣松 吴亚林 王亚云 鲍力伟  
(山东科技大学化学与环境工程学院, 青岛 266590)

**摘要:** 采用苯乙烯微球为模板水热合成了直径为 1~2  $\mu\text{m}$ , 管壁厚度约 200 nm 的 ZnO 管。用 SEM 和 XRD 对制得的样品进行表征, 结果表明, 醋酸锌浓度和水热时间在 ZnO 管的制备过程中起到重要作用。在实验结果的基础上, 提出了 ZnO 管的形成机理。紫外-可见吸收光谱计算出 ZnO 管的禁带宽度为 2.96 eV, 合成的 ZnO 管对罗丹明 B 具有很高的紫外光催化活性。

**关键词:** ZnO 管; 苯乙烯乳液; 模板; 光催化性能

中图分类号: 0614.24+1 文献标识码: A 文章编号: 1001-4861(2014)11-2601-06

DOI: 10.11862/CJIC.2014.375

## Polystyrene-Assisted Hydrothermal Preparation of ZnO Tubes with High Photocatalytic Activity

SHAO Qian\* YANG Meng-Chen GE Sheng-Song WU Ya-Lin WANG Ya-Yun BAO Li-Wei  
(College of Chemical and Environmental Engineering, Shandong University of Science & Technology, Qingdao, Shandong 266590, China)

**Abstract:** ZnO tubes with diameter of 1~2  $\mu\text{m}$  and wall thickness of *ca.* 200 nm were synthesized by a simple hydrothermal method using polystyrene (PS) microspheres as the template. Results from SEM and XRD show that the concentration of zinc acetate and hydrothermal time plays an important role in the formation of ZnO tubes. The growth mechanism is proposed. The band gap value calculated from a UV-Vis absorption spectrum of ZnO tubes is 2.96 eV. The as-synthesized ZnO tubes exhibit high photocatalytic activity for the photodegradation of Rhodamine B under UV-light irradiation.

**Key words:** ZnO tubes; PS latex; template; photocatalytic activity

### 0 Introduction

Recently, dye effluents from textile industries have been a more and more serious environmental problem because of their difficulty to chemical or biological degradation<sup>[1]</sup>. Semiconductors with wide band gap are widely used as photocatalysts for the degradation<sup>[2]</sup>. Of them,  $\text{TiO}_2$  and ZnO are extensively studied materials for their high photosensitivity and large band gap<sup>[3-5]</sup>. Due to the lower cost and higher photocatalytic activity than  $\text{TiO}_2$  in some cases, ZnO

draws more and more attention.

ZnO is a II-VI semiconductor with a wide direct band gap (3.37 eV) and a high electron-hole binding energy (60 mV) at room temperature<sup>[6]</sup>, and it has outstanding performance in the field of photocatalysis<sup>[7]</sup>. Various kinds of nanostructured ZnO such as nano hollow spheres<sup>[8]</sup>, nanorod<sup>[9]</sup>, nanosheet<sup>[10]</sup>, nanoplate<sup>[11]</sup>, and other micro/nanostructure have been fabricated for photocatalytic decomposition of the dye effluents. Among these ZnO structures, the preparation of ZnO with hollow structures has attracted a great deal of

收稿日期: 2014-03-26。收修改稿日期: 2014-09-13。

\*通讯联系人。E-mail: shaoqian01@126.com

attention due to their advantages of low density, high surface-to-volume ratio and their hollow structure in the photocatalytic progress<sup>[12-13]</sup>. Until now, the soft templates or hard templates methods are the most effective way to prepare ZnO with hollow structures<sup>[14]</sup>, and the widely used templates include silica spheres<sup>[15]</sup>, polymethacrylate (PMMA)<sup>[16]</sup>, polystyrene (PS)<sup>[17]</sup>, carbon spheres<sup>[14]</sup>, and so on. Dong et al<sup>[18]</sup> prepared series of multishelled ZnO hollow microspheres with controlled shell number and inter-shell spacing by a simple carbonaceous microsphere templating method, and the ZnO hollow structure realized a high conversion efficiency up to 5.6% when used in dye-sensitized solar cells. Deng et al<sup>[19]</sup> prepared ZnO hollow spheres using PS as the template, and ZnO hollow spheres have good photocatalytic activity. Zhang et al<sup>[20]</sup> reported the ZnO hollow nanofibers with diameters of 120 ~150 nm by electrospinning the precursor solution consisting of polyacrylonitrile, polyvinylpyrrolidone, and zinc acetate composite through a facile single capillary method, and the template role for preparing ZnO hollow nanofibers was investigated.

Despite many investigations about the preparation of ZnO with hollow structures, there are only few studies on the effective preparation of ZnO tubes by the PS template-assisted hydrothermal method. In this work, a facile hydrothermal method by using PS microspheres as the template was employed to synthesize ZnO tubes. The results show that the experimental parameters such as the concentration of  $\text{Zn}(\text{Ac})_2 \cdot 2\text{H}_2\text{O}$  and hydrothermal time have great influences on the formation of ZnO tubes. The photocatalytic activity of the as-prepared ZnO tubes was also examined.

## 1 Experimental

### 1.1 Materials

Potassium persulfate (KPS), zinc acetate ( $\text{Zn}(\text{Ac})_2 \cdot 2\text{H}_2\text{O}$ ) and absolute ethanol were purchased from Tianjin Benchmark Chemical Reagent Co. Ltd. (Tianjin, China). Styrene (St) and ethylenediamine were provided by Tianjin Bodi Co. Ltd. (Tianjin,

China). Rhodamine B (RhB) was purchased from Shanghai Chemical Reagent Co. Ltd. (Shanghai, China). All chemical reagents used were analytical grade and used without any further purification except that styrene was washed by 5wt% sodium hydroxide solution. Distilled water was used throughout.

### 1.2 Synthesis of PS latex

PS emulsion particles were prepared by emulsifier-free emulsion polymerization using KPS as anionic initiator. In a typical synthesis, under gentle stirring, 25 mL styrene and 200 mL distilled water were added into a 250 mL round flask in turn. After reacting for 15 min, 25 mL of KPS solution ( $1.6 \times 10^{-2} \text{ mol} \cdot \text{L}^{-1}$ ) was added into the round flask, the reaction temperature was controlled within 75 ~80 °C. The polymerization was continued with mechanical stirring at  $300 \text{ r} \cdot \text{min}^{-1}$  for 3 h and then samples were withdrawn at regular time and until the desired size was obtained.

### 1.3 Synthesis of ZnO tubes

In a typical hydrothermal process, ZnO tubes were fabricated using zinc acetate as a zinc source. 0.3 g zinc acetate was dissolved in 20 mL distilled water to form a homogeneous solution. Under magnetic stirring anhydrous ethylenediamine was then added into the solution until the pH value of 10. Afterwards, 10 mL of the above mixture was added dropwise into 15 mL of the as-obtained PS latex. After magnetic stirring for 10 min, the reaction solution was transferred into a 30 mL Teflon-lined stainless steel autoclave, followed by hydrothermal treatment at 160 °C for several hours. After hydrothermal reaction, the products were washed and centrifuged for 3 times with distilled water and absolute ethanol, and then dried at 100 °C for 2 h. Finally the products were annealed in air at 650 °C for 2 h to obtain the ZnO tubes.

### 1.4 Characterization

The morphologies of the ZnO tubes were observed by Scanning electron microscopes, (SU-70, Japan) with acceleration voltage of 30 kV. The crystal structure information of the prepared samples were analyzed by a X-ray diffraction (Rigaku D/Max2500PC, Japan) using  $\text{Cu } K\alpha$  radiation ( $\lambda = 0.154 \text{ nm}$ ) at a

scanning rate of  $4^{\circ} \cdot \text{min}^{-1}$  in  $2\theta$  range from  $20^{\circ}$ ~ $80^{\circ}$ . UV-Visible absorption spectra were recorded on a UV-Vis Spectrophotometer (Cary 500, Varian).

### 1.5 Photocatalytic activity test

The photocatalytic activity of the ZnO tubes was evaluated by the photodegradation of a model dye RhB. The experimental process was carried out as follows: 40 mg of the photocatalyst powder were dispersed in 30 mL of RhB aqueous solution ( $10 \text{ mg} \cdot \text{L}^{-1}$ ) in the beaker, and the suspensions were super-sonic treated for 30 min in the dark. The UV lamp with a wavelength of 254 nm was used as a light source and placed 10 cm above the beaker. After UV irradiation for 20 min, the reaction solution was filtered, and the absorption spectrum of the centrifuged solution was then recorded with a UV-Visible spectrophotometer (UV-3200PC, Shanghai).

## 2 Results and discussion

As indicated in the XRD pattern of Fig.1, three big peaks located at  $2\theta$  value of  $31.718^{\circ}$ ,  $34.439^{\circ}$  and  $36.261^{\circ}$  are indexed as (100), (002) and (101) planes

of wurtzite hexagonal structure ZnO (PDF No.36-1451), respectively. No peaks of metal Zn or any other phases are detected, indicating that the products are of high purity.

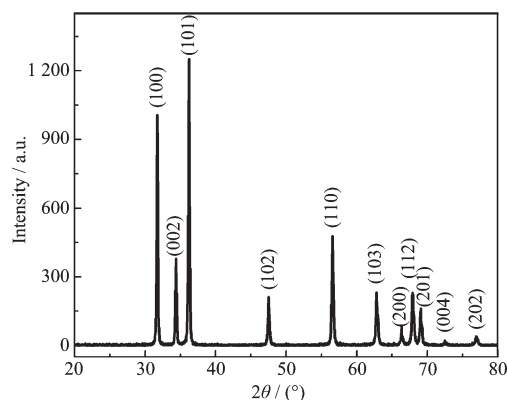


Fig.1 XRD pattern of the prepared ZnO tubes

SEM images of the PS template and ZnO tubes are shown in Fig.2. As shown in Fig.2a, the size of PS microspheres is uniform with an average particle size of 500 nm, and the microspheres with smooth surfaces are highly dispersed. Fig.2b~d show the SEM images of the as-prepared ZnO tubes, and the tubes are with

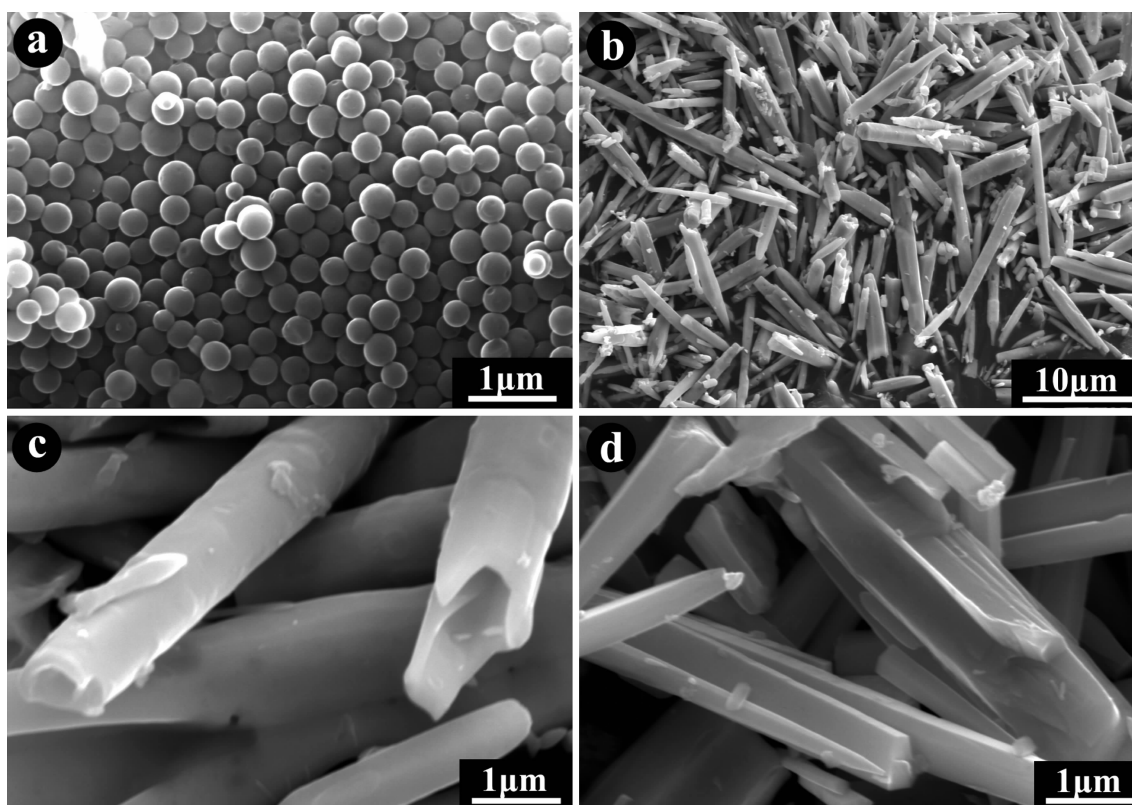


Fig.2 SEM images of (a) PS microspheres; (b) ZnO tubes; (c) an individual intact ZnO tube and (d) the broken ZnO tubes

a diameter of *ca.* 1~2  $\mu\text{m}$ , length of *ca.* 20  $\mu\text{m}$  and wall thickness *ca.* 200 nm. The hollow structure can be evidently viewed from an individual tube, as is shown in Fig.2c. The broken tubes (Fig.2d) are perhaps as a result of the escapement of  $\text{CO}_2$  during the calcinations.

The morphology of the ZnO tubes is affected by many factors such as  $\text{Zn}(\text{Ac})_2 \cdot 2\text{H}_2\text{O}$  concentration and hydrothermal time. Fig.3 shows a series of SEM images of as-obtained ZnO microstructures prepared with different  $\text{Zn}(\text{Ac})_2 \cdot 2\text{H}_2\text{O}$  concentrations while keeping other parameters unchanged. Irregular products (Fig.3a) are observed, when the concentration of zinc acetate is as low as  $0.04 \text{ mol} \cdot \text{L}^{-1}$ . In Fig.3b, high yield tubes are obtained when the concentration is  $0.07 \text{ mol} \cdot \text{L}^{-1}$ . Further increasing  $\text{Zn}(\text{Ac})_2 \cdot 2\text{H}_2\text{O}$  concentration to  $0.5 \text{ mol} \cdot \text{L}^{-1}$ , ZnO rodlike clusters are formed, as shown in Fig.3c.

In order to explore the shape evolution process of the ZnO tubes, the time-dependent experiments were carried out. A large number of globular aggregates with diameter of 20  $\mu\text{m}$  are formed with hydrothermal

treatment for 1 h. The too short hydrothermal time inhibits the oriented growth to obtain one dimensional nanomaterials. When the hydrothermal time is extended to 4 h (Fig.4b), the rods are formed. Further increasing the hydrothermal time to 12 h, ZnO with regular tubular structure is formed.

On the basis of the above information, the growth process of the ZnO tubes could be in four steps as shown in Fig.5. In the first step, the rheological properties of PS microspheres are changed with hydrothermal treatment, so some PS microspheres assemble together under high temperature and high pressure. Meanwhile, the  $\text{Zn}(\text{en})_2^{2+}$  is generated in the mixture of ethylene diamine and zinc acetate. In the second step, positive  $\text{Zn}(\text{en})_2^{2+}$  ions are captured by negative PS due to electrostatic adsorption. As shown in Fig.4a, a large number of globular aggregates with diameter *ca.* 20  $\mu\text{m}$  are formed under hydrothermal treatment for 1 h. In the third step, the samples grow along one direction with the guidance of the PS templates, and the rods gradually form with increase in hydrothermal time. Finally, the ZnO tubes are

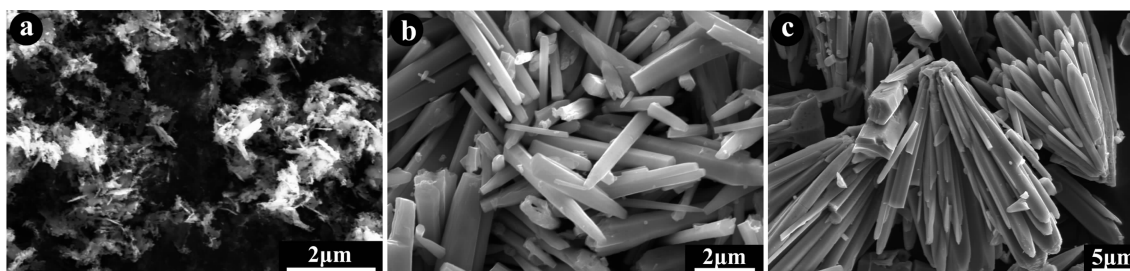


Fig.3 SEM images of the samples with different  $\text{Zn}(\text{Ac})_2 \cdot 2\text{H}_2\text{O}$  concentrations: (a)  $0.04 \text{ mol} \cdot \text{L}^{-1}$ ; (b)  $0.07 \text{ mol} \cdot \text{L}^{-1}$ ; (c)  $0.5 \text{ mol} \cdot \text{L}^{-1}$

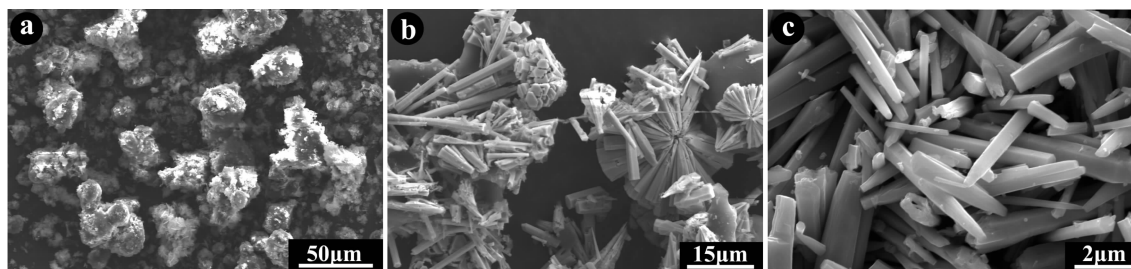


Fig.4 SEM images of the samples synthesized for different periods of hydrothermal time: (a) 1 h, (b) 4 h, (c) 12 h

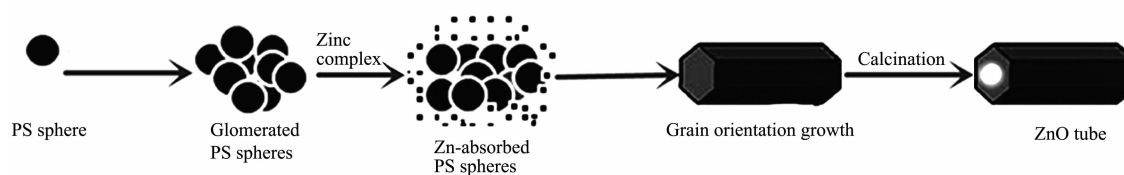


Fig.5 Formation mechanism of ZnO tubes using the PS microspheres as the template



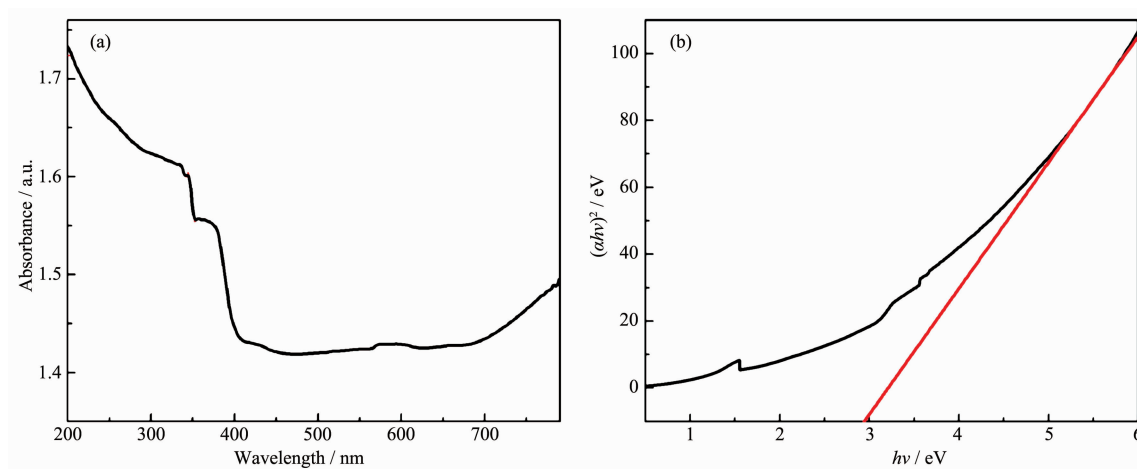


Fig.6 UV-Vis absorption spectrum (a) and the  $(\alpha h\nu)^2$  vs  $h\nu$  curve (b) of the ZnO tubes

successfully prepared by removing of the PS templates under calcination at 650 °C for 2 h.

UV-Vis absorption spectra of the samples are shown in Fig.6. The spectrum in Fig.6a shows that ZnO tubes absorb mainly the ultraviolet light with a wavelength below 420 nm. The equation  $(\alpha h\nu)^2 = K(h\nu - E_g)$  could be used to calculate the band gap of the samples, where  $\alpha$  is the absorption coefficient,  $\nu = c/\lambda$ ,  $h$  is Planck constant,  $K$  is a proportionality constant, and  $E_g$  is the band-gap energy. In Fig.6b, the extrapolated value (the straight lines to the  $x$ -position) shows the band gap of ZnO tubes is 2.96 eV. The results indicate that the prepared ZnO tubes may benefit their potential applications in organic pollutants degradation.

Fig.7 shows the degradation rate of RhB with or without ZnO tubes catalyst. For comparison, the

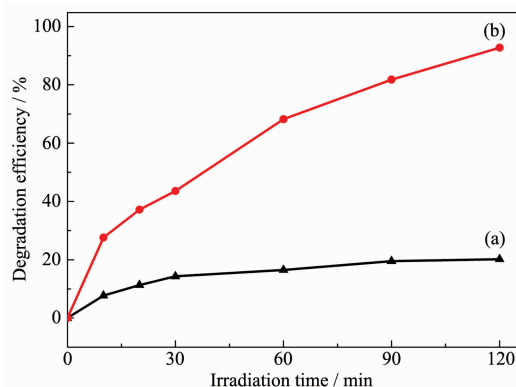


Fig.7 Degradation curves of RhB solution (a) without photocatalysts and (b) with ZnO tubes as photocatalysts under UV light irradiation

degradation rate of the RhB without any photocatalysts is no more than 20%, while the degradation over the ZnO tubes is 93%. The results indicate that the ZnO tubes show high photocatalytic decomposition of the dye, and the ZnO tubes may also have great potential application in the solar cells and photocatalytic decomposition of water to hydrogen.

### 3 Conclusions

In summary, we report here a method to synthesize ZnO tubes by a simple hydrothermal method using PS microspheres as the template. The morphology of the ZnO tubes can be influenced by the concentration of  $\text{Zn}(\text{Ac})_2 \cdot 2\text{H}_2\text{O}$  and hydrothermal time. A formation mechanism of the ZnO tubes is proposed. Meanwhile the as-prepared ZnO tubes exhibit high photocatalytic activity for the degradation of organic dye RhB under the UV illumination.

### References:

- [1] Yanagisawa K, Ovenstone J. J. *Phys. Chem. B*, **1999**,**103**: 7781-7787
- [2] Hoffmann M R, Martin S T, Choi W, et al. *Chem. Rev.*, **1995**,**95**:69-96
- [3] Linsebigler A L, Lu G, Yates J T. *Chem. Rev.*, **1995**,**95**:735-758
- [4] Jing L Q, Wang D J, Wang B Q, et al. *J. Mol. Catal. A*, **2006**,**244**:193-200
- [5] Stroyuk A L, Shvalagin V V, Kuchmii S Y. *Photochem. Photobiol. A*, **2005**,**173**:185-194

- [6] Cho S, Kim S, Lee K H. *J. Colloid Interface Sci.*, **2011**,**361**: 436-442
- [7] Li Y Z, Xie W, Hu X L, et al. *Langmuir*, **2010**,**26**:591-597
- [8] Yu J G, Yu X X. *Environ. Sci. Technol.*, **2008**,**42**:4902-4907
- [9] Jang E S, Won J H, Hwang S J, et al. *Adv. Mater.*, **2006**,**18**: 3309-3312
- [10] Lu F, Cai W P, Zhang Y G. *Adv. Funct. Mater.*, **2008**,**18**: 1047-1056
- [11] Ye C H, Bando Y, Shen G Z, et al. *J. Phys. Chem. B*, **2006**, **110**:15146-15151
- [12] Wang X, Hu P, Yuan F L, et al. *J. Phys. Chem. C*, **2007**, **111**:6706-6712
- [13] Duan J X, Huang X T, Wang E K, et al. *Nanotechnology*, **2006**,**17**:1786-1790
- [14] Lou X W, Archer L A, Yang Z C. *Adv. Mater.*, **2008**,**20**:1-33
- [15] Wang Y, Yu A, Caruso F. *Angew. Chem. Int. Ed.*, **2005**, **117**:2948-295
- [16] Peng B, Tang F, Chen D. *Colloid Interface Sci.*, **2009**,**329**: 62-66
- [17] Shao Q, Wang L Y, Wang X J. *Solid State Sci.*, **2013**,**20**:29-35
- [18] Dong Z H, Lai X Y, Halpert J E, et al. *Adv. Mater.*, **2012**, **24**:1046-1049
- [19] Deng Z W, Chen M, Gu G X, et al. *J. Phys. Chem. B*, **2008**, **112**:16-22
- [20] Zhang Z Y, Li X H, Wang C H, et al. *J. Phys. Chem. C*, **2009**,**113**:19397-19403